

COFREEVLA: COLLISION-FREE DUAL-ARM MANIPULATION VIA VISION-LANGUAGE-ACTION MODEL AND RISK ESTIMATION

Xuanran Zhai³, Binkai Ou², Yemin Wang⁴, Hui Yi Leong⁵, Qiaojun Yu⁶, Ce Hao³, Yaohua Liu^{1*}

¹ Guangdong Institute of Intelligence Science and Technology, ² BoardWare Information System Co.Ltd,
³ National University of Singapore, ⁴ Xiamen University, ⁵ University of Chicago,
⁶ Shanghai AI Lab, * corresponding to liuyaohua@gdiist.cn

ABSTRACT

Vision–Language–Action (VLA) models enable instruction-following manipulation, yet dual-arm deployment remains unsafe due to under-modeled self-collisions between arms and grasped objects. We introduce CoFreeVLA, which augments an end-to-end VLA with a short-horizon self-collision risk estimator that predicts collision likelihood from proprioception, visual embeddings, and planned actions. The estimator gates risky commands, recovers to safe states via risk-guided adjustments, and shapes policy refinement for safer rollouts. It is pre-trained with model-based collision labels and post-trained on real-robot rollouts for calibration. On five bimanual tasks with the PiPER robot arm, CoFreeVLA reduces self-collisions and improves success rates versus RDT and APEX.

Index Terms— Robot Manipulation, Vision-Language-Action Model, Collision Avoidance

1. INTRODUCTION

Vision–Language–Action (VLA) models have recently emerged as a powerful paradigm for robotic control, demonstrating remarkable capabilities in grounding natural language instructions into visual observations and executable actions [1, 2, 3, 4, 5]. While these models have shown impressive generalization in single-arm manipulation tasks, extending them to dual-arm systems introduces new challenges. Dual-arm manipulation requires coordination across two high-degree-of-freedom manipulators, making spatial reasoning and safety-critical planning considerably more complex [6, 7, 8]. Existing approaches largely focus on avoiding external collisions with the environment or task objects—via classical trajectory optimization and widely deployed toolchains—yet self-collisions between the two arms or between an arm and a grasped object remain underexplored in end-to-end VLA settings [9, 10, 11, 12, 13, 14, 15]. Such self-collisions can result in task failure, hardware damage, or unsafe behaviors, and therefore pose a fundamental obstacle to deploying VLA-based dual-arm systems in real-world environments.

To address this gap, we propose **CoFreeVLA**, a risk-aware VLA framework designed for collision-free dual-arm manipulation. At the core of CoFreeVLA is a self-collision risk estimator that predicts the likelihood of future colli-

sions given the current observation and planned actions from the VLA policy. This risk estimator is integrated into the control loop in three complementary ways: (i) by halting unsafe actions before collisions occur, (ii) by guiding the system to recover toward safe configurations when risk is detected, and (iii) by refining the VLA policy itself through optimization with risk-aware feedback. By embedding explicit collision reasoning into VLA decision-making—complementary to classical safety layers such as control barrier functions [16, 17]—CoFreeVLA enables safer and more reliable dual-arm manipulation without sacrificing task performance.

We evaluate CoFreeVLA across a set of dual-arm manipulation tasks that highlight the need for safe spatial reasoning, including handover, cooperative grasping, and assembly [18, 19, 20]. To train and validate the risk estimator, we employ a two-stage strategy: pre-training with synthetic collision data generated from a model-based checker [13, 11, 12], followed by post-training with real-robot rollouts under VLA policies. Our experiments assess both the predictive accuracy of the risk estimator and the downstream benefits of risk-aware policy refinement. We benchmark CoFreeVLA against recent dual-arm learning baselines, including APEX and RDT-1B [21, 22], on an AgileX-based dual-arm platform [23], measuring performance in terms of task success, collision rate, and recovery effectiveness.

In summary, this work makes the following contributions: **(1)** We propose CoFreeVLA, a framework that addresses the overlooked problem of inter-arm and arm–object collision in dual-arm VLA-based manipulation. **(2)** We design a self-collision risk estimator that predicts collision likelihood from visual observations and action sequences, and integrate it into execution, recovery, and policy refinement. **(3)** We conduct extensive experiments on dual-arm manipulation tasks, validating the effectiveness of CoFreeVLA in reducing risky collisions while maintaining task performance.

2. RELATED WORKS

Vision-Language-Action (VLA) models. VLA models couple internet-scale vision-language pretraining with robot action policies to follow natural-language instructions from raw images. RT-2 showed end-to-end VLA transfer from web knowledge to real robots [1]. PaLM-E unified visual, language, and proprioceptive inputs for embodied reason-

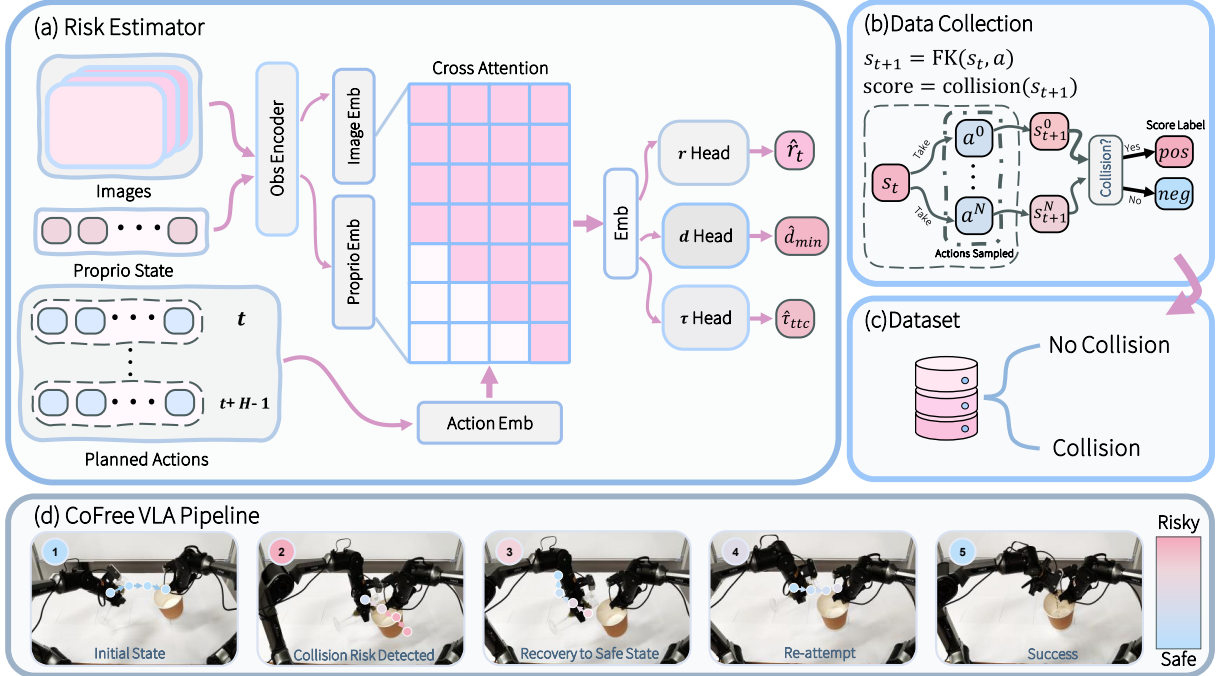


Fig. 1. (a) Risk Estimator. Given a state–action pair, the model applies a cross-attention module followed by three heads to predict collision risk r , minimum distance d , and time-to-collision τ . **(b) Data Collection** and **(c) Dataset.** For each state, we sample candidate actions and check their outcomes for labeling. **(d) CoFree VLA.** At run time, the system continuously estimates risk; when it exceeds a threshold, the policy will be blocked and the arms will be returned to a safe configuration, after which the policy resumes to complete the task.

ing and manipulation [2]. Building on large, heterogeneous robot datasets, Octo introduced an open generalist policy trained on Open X-Embodiment trajectories with efficient finetuning to new sensors and action spaces [3]. OpenVLA further provided an open 7B VLA trained on $\sim 970k$ robot episodes, enabling quick adaptation across platforms [4]. Earlier SayCan demonstrated LLM-guided skill selection via affordances, a precursor to modern VLA pipelines [5]. These works establish strong instruction-following and generalization but typically rely on dataset priors or standard planners for safety, without explicit self-collision prediction for dual-arm settings.

Collision avoidance for robot manipulation. Classical motion planning enforces collision constraints via geometric models and trajectory optimization—e.g., CHOMP for functional-gradient trajectory refinement [9], and TrajOpt via sequential convex optimization with convexified collision checking [10]—and is widely deployed in toolchains like MoveIt/OMPL for fast self-collision checks [11, 12]. Beyond planning, control barrier functions (CBFs) provide real-time safety filters that guarantee set invariance at the controller level [17, 16]. For dual-arm systems, research targets mutual-arm interference and self-collision through specialized planners and reactive controllers, including kinematics-based real-time self-collision avoidance with bounding-volume models [14], coordinated dual-arm motion planning frame-

works [15], and recent learning-based approaches such as APEX, which learns collision-free latent motion for ambidextrous dual-arm manipulation [21]. However, predicting imminent self-collision directly from observations and planned action sequences and integrating this prediction into a VLA policy loop remains underexplored—precisely the gap our risk-aware CoFreeVLA addresses.

3. METHOD

Problem formulation. We consider a dual-arm manipulator with left/right degrees of freedom n_L, n_R . The joint configuration at time t is $q_t = (q_t^L, q_t^R) \in \mathbb{R}^{n_L+n_R}$ (subject to joint and velocity limits). Each arm has end-effector pose $x_t^k \in SE(3)$ and gripper state g_t^k for $k \in \{L, R\}$. Actions are Cartesian end-effector increments $\Delta x_t = (\Delta x_t^L, \Delta x_t^R)$; we denote the control command by $a_t \equiv \Delta x_t$. The decision state is $s_t = (x_t, g_t, o_t)$, where o_t includes onboard perception (e.g., RGB-D) and the task instruction. An end-to-end vision–language–action policy maps images, language, and proprioception to executable actions, written $a_t \sim \pi_\theta(\cdot | s_t)$ or concretely $a_t = f_\theta(s_t)$.

3.1. Self-Collision Risk Estimator

Inputs–outputs. As in Fig. 1(a), the estimator takes the current dual-arm state and a short-horizon plan as input. We form the action sequence $A_{t:t+H-1} = (a_t, \dots, a_{t+H-1})$

from the VLA policy, pair it with proprioceptive state (x_t, g_t) , and a visual embedding $z_t = f_{\text{VLA}}(o_t)$ from the VLA backbone. The estimator predicts a calibrated self-collision risk $\hat{r}_t = E_\phi(x_t, g_t, z_t, A_{t:t+H-1}) \in [0, 1]$ and optionally geometric surrogates such as the minimum inter-body distance \hat{d}_{min} (mm) and time-to-collision $\hat{\tau}_{\text{ttc}}$ (s), produced by auxiliary heads. We target inter-arm and arm-grasped-object collisions; environment collisions are handled by a separate module.

Network structure. We tokenize inputs into (i) a proprio/action stream and (ii) a vision stream. The proprio/action stream encodes (x_t, g_t) together with $A_{t:t+H-1}$ as a length- H token sequence with positional encodings; the vision stream provides a compact feature z_t taken from the penultimate VLA image token. A lightweight temporal encoder (MLP for small H , or a small Transformer for $H \geq 5$) fuses the two streams via cross-attention, followed by pooling and prediction heads for \hat{r}_t , \hat{d}_{min} , and $\hat{\tau}_{\text{ttc}}$. We apply temperature scaling to calibrate \hat{r}_t , and size the network for sub-5 ms inference so it can run at control rates (10–50 Hz).

Training data and collection. In Fig. 1(b)(c), we construct a dataset $\mathcal{D} = \{(x_t, g_t, z_t, A_{t:t+H-1}, y_t)\}_{t=1}^N$ with labels $y_t = \{y_t^{\text{bin}}, y_t^d, y_t^{\text{ttc}}\}$. *Pre-train:* using a model-based checker (e.g., mesh-distance), we roll out candidate $A_{t:t+H-1}$ from the VLA (with jitter) and record a binary collision-within- H indicator $y_t^{\text{bin}} \in \{0, 1\}$, the minimum inter-arm/arm-object distance y_t^d , and the first time-to-collision y_t^{ttc} . We emphasize near-collision cases by oversampling small y_t^d . *Post-train:* on real-robot roll-outs, we re-label with contact events, torque spikes, and vision overlap to account for calibration and grasp uncertainties. The loss combines BCE for y_t^{bin} (with higher weight on false negatives) and regression for y_t^d, y_t^{ttc} : $\mathcal{L} = \lambda_{\text{bce}} \text{BCE}(\hat{r}_t, y_t^{\text{bin}}) + \lambda_d \|\hat{d}_{\text{min}} - y_t^d\|_2^2 + \lambda_{\text{ttc}} \|\hat{\tau}_{\text{ttc}} - y_t^{\text{ttc}}\|_1$, with optional early-collision weighting (e.g., $\gamma^{y_t^{\text{ttc}}}$) and temperature calibration on a held-out set.

3.2. Collision-Free VLA Structure

Risk estimation to stop. In Fig. 1(d), at each control step, the VLA proposes a short-horizon plan $A_{t:t+H-1} = (a_t, \dots, a_{t+H-1})$. We evaluate the self-collision risk $\hat{r}_t = E_\phi(s_t, A_{t:t+H-1}) \in [0, 1]$. If $\hat{r}_t > \tau_\uparrow$, execution of a_t is blocked and the controller enters a protective mode; execution resumes only when $\hat{r}_t \leq \tau_\downarrow$ (hysteresis with $\tau_\downarrow < \tau_\uparrow$ reduces chattering). As an optional soft gate when not blocked, commanded velocities are scaled by $\alpha_t = \text{clip}(1 - \hat{r}_t/\tau_\uparrow, 0, 1)$ before sending to the low-level controller.

Recovery to safe states. When blocked, we synthesize a short recovery sequence $A_{t:t+h-1}^{\text{rec}}$ that drives the system toward the self-safe set $\mathcal{S}_{\text{safe}} = \{q : d_{\text{min}}(q) \geq d_0\}$. We optimize a risk-shaped objective $A_{t:t+h-1}^{\text{rec}} \leftarrow \arg \min_A E_\phi(s_t, A) + \lambda \|A\|^2$ under joint and velocity limits, solved by a few projected-gradient steps. This locally reduces predicted collision risk; recovery terminates once

$\hat{r}_t \leq \tau_\downarrow$ for K consecutive cycles.

Policy optimization for collision-free control. Beyond online gating, we fine-tune the VLA with a safety-aware objective that trades off task intent against predicted risk. We minimize a surrogate that keeps the refined plan close to the original while lowering E_ϕ : $\min_\theta \mathbb{E}_{s_t} [\alpha \|A'_{t:t+H-1} - A_{t:t+H-1}\|^2 + \beta E_\phi(s_t, A'_{t:t+H-1})]$, where $A'_{t:t+H-1}$ is obtained by rolling out $f_\theta(s_t)$ for H steps. Practically, we perform (i) supervised fine-tuning on a filtered dataset $\mathcal{D}_{\text{safe}} = \{(s, a) : E_\phi(s, A_{t:t+H-1}) \leq \tau_\downarrow\}$ with risk-weighted losses $w(s) = \exp(-\kappa E_\phi(s, A_{t:t+H-1}))$, biasing the model toward a collision-free target distribution; and (ii) test-time action refinement by solving $\min_{A'} \alpha \|A' - A_{t:t+H-1}\|^2 + \beta E_\phi(s_t, A')$ under control limits, then executing only the first optimized step to preserve reactivity. This balances task success with collision-free behavior.

3.3. Collision-free VLA Training

Risk estimator pre-training. We first train E_ϕ offline using model-based collision labels. From states s_t , we sample horizon plans $A_{t:t+H-1}$ by rolling out the base VLA with jitter and beam variants in simulation and on the real robot in guard mode. For each $(s_t, A_{t:t+H-1})$ we compute labels via mesh-distance queries (inter-arm and arm-grasped-object) and a predictive checker to obtain: (i) a binary event $y_t^{\text{bin}} \in \{0, 1\}$ indicating collision within H , (ii) the minimum distance y_t^d (mm) over the horizon, and (iii) the first time-to-collision y_t^{ttc} (s). The training loss combines calibrated BCE and regression: $\mathcal{L} = \lambda_{\text{bce}} \text{BCE}(\hat{r}_t, y_t^{\text{bin}}) + \lambda_d \|\hat{d}_{\text{min}} - y_t^d\|_2^2 + \lambda_{\text{ttc}} \|\hat{\tau}_{\text{ttc}} - y_t^{\text{ttc}}\|_1$, with class-imbalance handling and *false-negative* upweighting. We emphasize near-miss samples by oversampling small y_t^d and curriculum the horizon H (start short, then grow). After training, we apply temperature scaling on a held-out set to calibrate $\hat{r}_t \in [0, 1]$.

Closed-loop fine-tuning. We adapt both E_ϕ and the VLA in a safety-supervised loop. Deploy with the risk gate $(\tau_\uparrow, \tau_\downarrow)$ enabled; collect tuples $(s_t, A_{t:t+H-1}, \hat{r}_t)$, contact events, and corrected actions from the recovery controller. Aggregate data in a DAGger-like buffer and (i) *post-train* E_ϕ on real-robot labels to account for calibration and grasp uncertainty, and (ii) *refine* the VLA with a risk-weighted objective, $\min_\theta \mathbb{E}_{(s,a) \sim \mathcal{D}} [\ell_{\text{BC}}(\pi_\theta(s), a) w(s)]$, where $w(s) = \exp(-\kappa E_\phi(s, A_{t:t+H-1}))$. Optionally add pairwise preferences (safe vs. unsafe variants) or a small RL term with a risk penalty. Thresholds are tuned via ROC analysis prioritizing low false negatives; hysteresis avoids chatter, and a watchdog halts if \hat{r}_t saturates.

System implementation. We run the VLA [22] at 10 Hz and the low-level controller at 30 Hz. At each step, the VLA proposes $A_{t:t+H-1}$ (typically $H=5 \sim 10$); we batch N candidates (beam + jitter) through E_ϕ and execute the first action from the lowest-risk feasible sequence. If $\hat{r}_t > \tau_\uparrow$, we enter recovery: gradient-based action refinement (when E_ϕ is differentiable) or a QP/CBF fallback using the distance head;



Fig. 2. Experimental results in 5 dual-arm manipulation tasks. Evaluation of collision and success rates is on 10 trials.

execution resumes when $\hat{r}_t \leq \tau_{\downarrow}$ for K cycles. For geometric supervision we use link meshes (inflated to cover grasped-object uncertainty) and fast distance queries; for runtime efficiency we export E_{ϕ} to ONNX/TorchScript, keep the model small (sub-5 ms forward on CPU/GPU), and prefetch z_t from the VLA backbone to keep the loop within the control budget.

4. EXPERIMENT

In this section, we evaluate CoFreeVLA on real-robot bimanual manipulation under realistic constraints. We ask three questions: (1) *Risk prediction* — can the estimator anticipate imminent inter-arm and arm-object collisions from the current state and a short-horizon plan? (2) *Safety impact* — does risk-aware gating and recovery measurably reduce self-collision events during execution? (3) *Task performance* — does CoFreeVLA improve success rate over strong baselines while keeping latency and episode time within acceptable limits?

Experimental setup. We collect demonstrations and train all policies on a Piper-style bimanual mobile manipulator [19]. We evaluate five real-robot bimanual tasks, with aggregated results in Figure 2. Under a common protocol (identical prompts, sensing, and resets), we compare RDT-1B [22], APEX [21], and CoFreeVLA, reporting two metrics: (i) collision rate (fraction of trials with self-collision) and (ii) overall task success rate.

4.1. Self-Collision Risk Estimation

Across the five tasks in Figure 2, outcomes split into two regimes. In the high inter-arm interference case (*Pouring Beans*), CoFreeVLA sharply lowers collisions (RDT 8/10 \rightarrow 2/10, APEX 6/10 \rightarrow 2/10), showing that short-horizon risk with gating/recovery is effective when arms must cross. On precision tasks—*Pen Cap Removal*, *Tool Handover*, *Tubes Placement*, *Cups Nesting*—baselines rarely

collide (1/10), while our current calibration yields higher rates (4/10, 3/10, 2/10, 5/10). These errors stem from conservative thresholds, false negatives near contact transitions, and occasional recovery oscillations. Overall, CoFreeVLA reduces collisions where interference is intrinsic, and points to tighter post-training calibration plus horizon/threshold tuning to suppress residual events on fine-alignment tasks.

4.2. Collision-Free VLA

End-to-end, risk-gated execution shows the same pattern. In interference-prone geometry (*Pouring Beans*), CoFreeVLA prevents many wrist-wrist and arm-object strikes (RDT 8/10 \rightarrow 2/10, APEX 6/10 \rightarrow 2/10). On precision tasks with already low baseline collisions, current settings yield higher counts (4/10, 3/10, 2/10, 5/10), driven by occasional false negatives and recovery re-approach. Task success is comparable across methods (all 1/10 in this study). Added latency from risk inference is negligible (sub-5 ms/tick), and blocked-step fraction stays within budget via hysteresis with $\tau_{\downarrow} < \tau_{\uparrow}$. In sum, CoFreeVLA improves safety where self-interference dominates and requires modest calibration and H /threshold tuning to extend gains to precision regimes.

5. CONCLUSION

Vision-Language-Action models enable instruction-following manipulation, but dual-arm use remains risky due to under-modeled self-collisions. We introduced **CoFreeVLA**, which augments a VLA with a short-horizon self-collision estimator to gate unsafe actions, recover to safe states, and refine proposals, trained via model-based pre-training and real-robot post-training and operating in real time. Across five bimanual tasks, CoFreeVLA reduces self-collisions and preserves efficiency, outperforming strong baselines in interference-prone settings and demonstrating that explicit short-horizon risk reasoning enables safer dual-arm VLA manipulation.

6. COMPLIANCE WITH ETHICAL STANDARDS

This study involves robotic experiments only. No human participants, personal data, or animals were involved. Therefore, no ethical approval was required.

7. REFERENCES

- [1] A. Brohan et al., “Rt-2: Vision-language-action models transfer web knowledge to robotic control, 2023,” *URL* <https://arxiv.org/abs/2307.15818>, 2024.
- [2] D. Driess et al., “Palm-e: An embodied multimodal language model,” 2023.
- [3] Octo Model Team et al., “Octo: An open-source generalist robot policy,” *arXiv preprint arXiv:2405.12213*, 2024.
- [4] M. Kim et al., “Openvla: An open-source vision-language-action model,” *arXiv preprint arXiv:2406.09246*, 2024.
- [5] M. Ahn et al., “Do as i can, not as i say: Grounding language in robotic affordances,” *arXiv preprint arXiv:2204.01691*, 2022.
- [6] Mohamed Abbas, Jyotindra Narayan, and Santosha K Dwivedy, “A systematic review on cooperative dual-arm manipulators: modeling, planning, control, and vision strategies,” *International Journal of Intelligent Robotics and Applications*, vol. 7, no. 4, pp. 683–707, 2023.
- [7] Jianxin Bi, Kevin Yuchen Ma, Ce Hao, Mike Zheng Shou, and Harold Soh, “Vla-touch: Enhancing vision-language-action models with dual-level tactile feedback,” *arXiv preprint arXiv:2507.17294*, 2025.
- [8] Xuanran Zhai and Ce Hao, “Vfp: Variational flow-matching policy for multi-modal robot manipulation,” *arXiv preprint arXiv:2508.01622*, 2025.
- [9] M. Zucker et al., “Chomp: Covariant hamiltonian optimization for motion planning,” *The International journal of robotics research*, vol. 32, no. 9-10, pp. 1164–1193, 2013.
- [10] J. Schulman et al., “Motion planning with sequential convex optimization and convex collision checking,” *The International Journal of Robotics Research*, vol. 33, no. 9, pp. 1251–1270, 2014.
- [11] MoveIt Tutorials, “Ompl planner — collision/self-collision checking,” .
- [12] MoveIt Docs, “Planning scene — self-collision checking,” .
- [13] Jia Pan, Sachin Chitta, and Dinesh Manocha, “Fcl: A general purpose library for collision and proximity queries,” in *2012 IEEE international conference on robotics and automation*. IEEE, 2012, pp. 3859–3866.
- [14] M. Lei et al., “Real-time kinematics-based self-collision avoidance algorithm for dual-arm robots,” *Applied Sciences*, vol. 10, no. 17, pp. 5893, 2020.
- [15] P. Fresnillo et al., “Extending the motion planning framework—moveit with advanced manipulation functions for industrial applications,” *Robotics and Computer-Integrated Manufacturing*, vol. 83, pp. 102559, 2023.
- [16] A. Ames et al., “Control barrier function based quadratic programs for safety critical systems,” *IEEE Transactions on Automatic Control*, vol. 62, no. 8, pp. 3861–3876, 2016.
- [17] A. Ames et al., “Control barrier functions: Theory and applications,” in *2019 18th European control conference (ECC)*. Ieee, 2019, pp. 3420–3431.
- [18] Markus Grotz, Mohit Shridhar, Yu-Wei Chao, Tamim Asfour, and Dieter Fox, “Peract2: Benchmarking and learning for robotic bimanual manipulation tasks,” in *CoRL 2024 Workshop on Whole-body Control and Bimanual Manipulation: Applications in Humanoids and Beyond*, 2024.
- [19] Z. Fu et al., “Mobile aloha: Learning bimanual mobile manipulation with low-cost whole-body teleoperation,” *arXiv preprint arXiv:2401.02117*, 2024.
- [20] Qiaojun Yu, Ce Hao, Junbo Wang, Wenhai Liu, Liu Liu, Yao Mu, Yang You, Hengxu Yan, and Cewu Lu, “Manipose: A comprehensive benchmark for pose-aware object manipulation in robotics,” *arXiv preprint arXiv:2403.13365*, 2024.
- [21] A. Dastider et al., “Apex: ambidextrous dual-arm robotic manipulation using collision-free generative diffusion models,” in *2024 IEEE/RSJ International Conference on Intelligent Robots and Systems (IROS)*. IEEE, 2024, pp. 9526–9533.
- [22] S. Liu et al., “Rdt-1b: a diffusion foundation model for bimanual manipulation,” *arXiv preprint arXiv:2410.07864*, 2024.
- [23] AgileX Robotics, “Agilex robotics — global,” .